

Determination of the Number and Location of the Manganese Binding Sites of DNA Quadruplexes in Solution by EPR and NMR in the Presence and Absence of Thrombin

Vasilios M. Marathias¹, Ke Yu Wang¹, Surat Kumar¹, Thy Q. Pham¹
S. Swaminathan² and Philip H. Bolton^{1*}

¹Chemistry Department
Wesleyan University
Middletown, CT 06459, USA

²Gilead Sciences
346 Lakeside Drive
Foster City, CA 94404, USA

The interaction of a DNA quadruplex with thrombin has been studied by first determining the sites of manganese binding to the quadruplex in the absence of thrombin. This has been followed by determining if the interactions with thrombin displace the bound manganese. A different DNA quadruplex has also been studied as a control.

The refined solution structures of two DNA quadruplexes have been used to predict the electrostatic potentials of these DNAs. The calculated electrostatic potentials have been used to predict the locations of the binding sites of the paramagnetic ion manganese to these DNAs. The enhanced relaxation of DNA protons due to the binding of the paramagnetic metal ion Mn^{2+} has been used to experimentally determine the locations of the binding sites. The NMR results and the predictions based on the electrostatic potentials both place the binding sites of the manganese in the narrow grooves of these quadruplex DNAs. The predicted locations are spatially close to those experimentally observed, and the predicted and experimental locations also have similar electrostatic potential energy. These results have allowed a validation of the predictions of electrostatic potentials from structure.

The 15mer quadruplex has two strong Mn^{2+} binding sites with one in each narrow groove. Both Mn^{2+} are released when the 15mer is complexed with thrombin, indicating that both narrow grooves are involved in the 15mer–thrombin interactions. The dimer quadruplex has a different structural motif than the 15mer and the presence of thrombin does not appreciably affect its interactions with Mn^{2+} .

© 1996 Academic Press Limited

Keywords: aptamer; DNA; electrostatics; metal binding; telomere; thrombin

*Corresponding author

Introduction

Oligonucleotides are polyelectrolytes and the importance of electrostatic interactions in determining the stabilities, structures, metal ion binding, protein interactions and other properties of nucleic acids has been recognized for quite some time (Granot *et al.*, 1982a,b; Manning, 1978; Record *et al.*, 1978). The examination of the structures of

DNA–protein complexes shows that there can be interactions between basic residues of the protein with the phosphates of the DNA, which are thought to contribute to the stability and specificity of the complexes.

Until a few years ago DNA quadruplex structures were primarily a curiosity. Recent studies have shown that DNA quadruplexes are important as lead molecules in drug design and as a structural motif adopted by telomere, fragile X and other naturally occurring DNAs. A quadruplex structure is formed by the sequence d(GGTTGGT-GTGGTTGG), which has been shown to bind to, and inhibit, thrombin and the structural

Abbreviations used: NMR, nuclear magnetic resonance; EPR, electron paramagnetic resonance; NOESY, nuclear Overhauser effect spectroscopy; rms, root mean square.

information obtained on this quadruplex is being used to design therapeutic drugs (Bock *et al.*, 1992; Griffin *et al.*, 1993a,b; Wang *et al.*, 1993a).

One aim is to determine if the formation of the thrombin–DNA complex affects the manganese binding of this DNA. If the binding sites of manganese to the free DNA are known, then the determination of whether thrombin binding blocks the binding sites can give information about the nature of the thrombin–DNA complex. The interactions of a different type of quadruplex with thrombin have been used as a control.

Here we present an examination of the electrostatic potentials and metal binding properties of two quadruplex DNAs. The structures of refined solution state of these DNAs have been determined and have been used to predict the electrostatic potentials of the DNAs. The electrostatic potentials have been used to predict the number and location of the binding sites of the paramagnetic ion manganese. The locations of the manganese binding sites have been experimentally determined *via* observation of the enhanced relaxation of protons induced by the paramagnetic manganese ion. Comparison of the experimental and predicted metal ion binding sites allows a check of the validity of the methods used to predict the electrostatic potentials from the solution state structures.

While the electrostatic potentials of duplex DNAs have been extensively studied, less is known about the potentials of many of the other structural forms that can be adopted by nucleic acids. Transfer RNA (tRNA) is known to have binding sites for metal ions that are much stronger than those of duplex DNA (Shimmel & Redfield, 1980). The tertiary structure of tRNA brings phosphate groups much closer together than is found in duplex DNA and this close proximity of phosphates is thought to give rise to the strong metal ion binding sites of tRNA (Shimmel & Redfield, 1980). RNA pseudoknot structures are known to be stabilized by the presence of magnesium (Wyatt *et al.*, 1990), though the binding constants and the number of binding sites of RNA pseudoknots have not been well characterized.

DNA and RNA can form a variety of types of quadruplex structures. DNA quadruplex structures may play roles in telomere structure and function, immunoglobulin switch regions, centromere DNA and other naturally occurring biological systems, as discussed (Aboul-ela *et al.*, 1992; Blackburn, 1994; Kang *et al.*, 1992; Sen & Gilbert, 1992; Smith & Feigon, 1992; Wang *et al.*, 1994; Williamson, 1993). The unusual structural and electrostatic properties of DNA quadruplexes may be involved in the biological activities of these DNAs. It is known that the DNA aptamer d(GGTTGGTGGTTGG), which binds to, and inhibits, thrombin adopts an intramolecular quadruplex structure that is depicted in Figure 1 (Wang *et al.*, 1993a). The tertiary structure of this DNA aptamer is preserved upon binding to thrombin (Wang *et al.*, 1993a) This

aptamer binds to the positively charged exosite of thrombin and there are presumably favorable interactions between the aptamer and several lysine residues at the exosite of thrombin.

The stability of quadruplex structures is known to be dependent on the nature and concentration of monovalent counterions (Hardin *et al.*, 1991, 1992; Ross & Hardin, 1994; Sen & Gilbert, 1990; Williamson *et al.*, 1989a,b). The results of these studies have indicated that the effects of monovalent ions on the properties of quadruplex DNA are quite different from the effects on those of duplex DNA, tRNA or pseudoknot RNA. There have been reports that certain divalent and trivalent ions can stabilize the quadruplex structures of DNA (Hardin *et al.*, 1992; Nagesh *et al.*, 1992). We have recently shown that manganese preferentially binds to the narrow grooves of two distinct types of quadruplex DNAs (Wang *et al.*, 1995).

Structural information on several types of DNA quadruplexes is now available. These structures include quadruplexes formed by parallel stranded tetramers (Aboul-ela *et al.*, 1992; Guschlbauer *et al.*, 1990; Laughlan *et al.*, 1994; Wang *et al.*, 1991, 1995; Wang & Patel, 1992), quadruplexes formed by dimers with the loops either crossing over in a basket type structure or as an edge dimer (Kang *et al.*, 1992; Scaria *et al.*, 1992; Smith & Feigon, 1992, 1993; Smith *et al.*, 1994; Wang & Patel, 1993) and quadruplexes formed by intramolecular folding (Macaya *et al.*, 1993; Wang *et al.*, 1993a,b). The bases forming a quartet can be all *anti*, as is the case for the parallel stranded structures, or *syn-anti-syn-anti* or *syn-syn-anti-anti*, as have been found for dimer and intramolecular structures as shown in Figure 1. In addition, both *syn-syn* and *syn-anti* alternation from 5' to 3' have been observed. These studies have shown that a wide range of quadruplex structural motifs is possible.

Here we are interested in the two distinct types of quadruplex structures that are illustrated in Figure 1. The DNA aptamer d(GGTTGGTGGTGG) forms an intramolecular quadruplex structure that is referred to as a chair. The DNA d(GGGTTTTGGGG) adopts a quadruplex structure formed of dimers as shown in Figure 1 and this type of structure is referred to as a basket. The electrostatic potentials of the basket and chair types of DNA quadruplexes are expected to be distinct, since the distribution of groove widths is quite different in the two cases. Figure 1 shows a depiction of the groove widths of a chair form DNA quadruplex in which the dG residues alternate *syn-anti-syn-anti*, and a basket form in which the dG residues alternate *anti-anti-syn-syn*. The depiction shows that chair structures have both narrow and wide grooves. The narrow grooves have a short phosphate–phosphate distance of about 7 to 9 Å, which is shorter than that of B-form DNA. A basket structure has three different width grooves, which are marked narrow, medium and wide. The narrow groove of a basket structure is also about 7 to 9 Å wide. The presence of the narrow grooves suggests

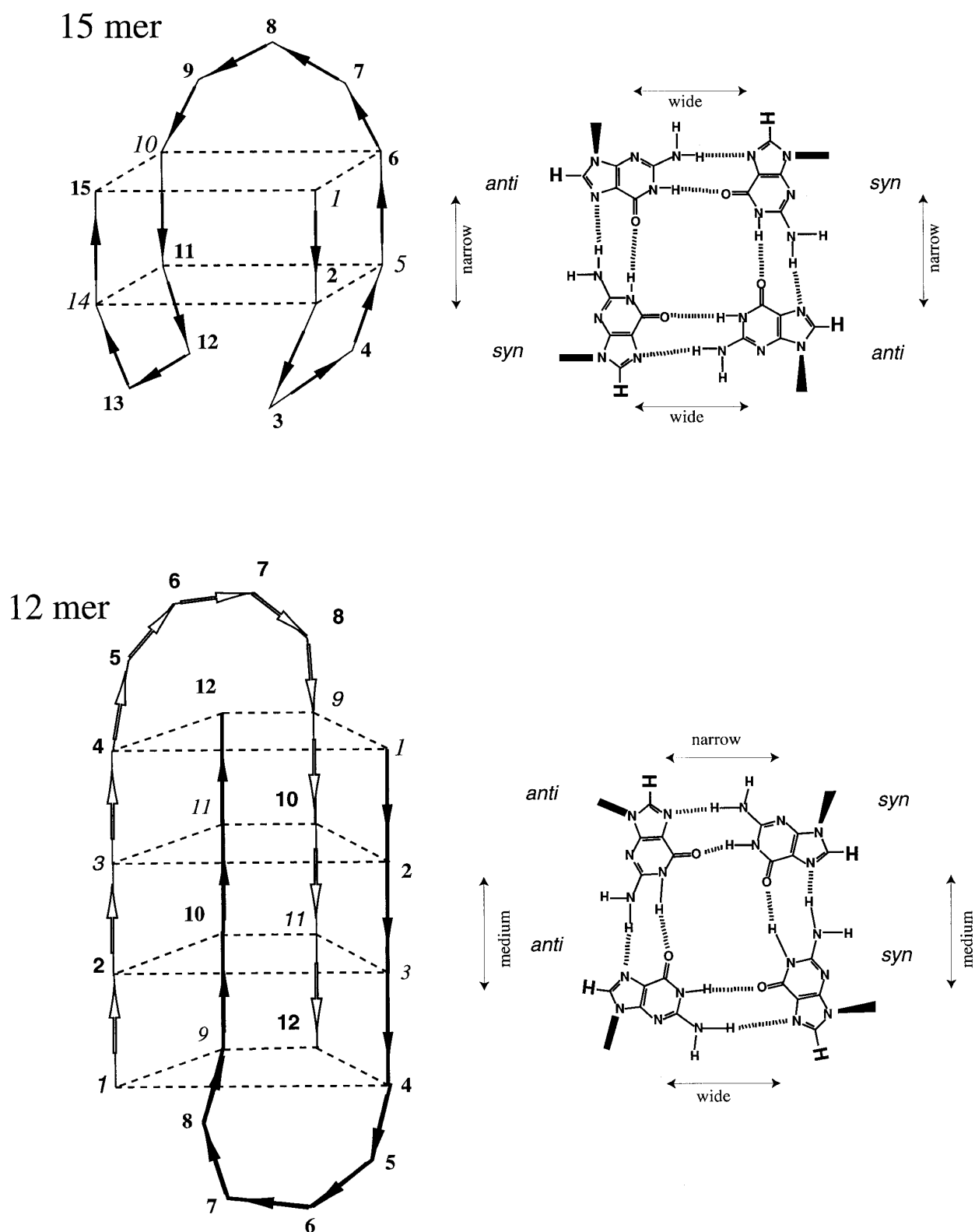


Figure 1. Schematic depictions of the quadruplex structures of the 15mer and of the 12mer. Also shown are depictions of the groove widths and base-pairing schemes associated with the two types of structures. For the 12mer the A strand is shown filled and the B strand is open.

that quadruplex DNAs may have very strong metal ion binding sites and that the binding sites of chair and basket structures may be discernibly distinct.

As shown below we have obtained the refined solution structures of both of these DNAs. These refined structures have been used to predict the electrostatic potentials, which in turn have been used to predict the locations of the binding sites of manganese ions. The locations of the Mn^{2+} binding sites have been determined from the paramagnetic-induced relaxation of the protons of the quadruplexes. Both quadruplexes have two strong binding sites in the narrow grooves. Comparison of the experimental and predicted binding sites offers a validation of the procedures for determination structure and electrostatic potential calculation. The information obtained on the free aptamer–manganese complex can then be used to interpret the results from experiments on the aptamer–thrombin complex. The complex of thrombin with the quadruplex formed by the dimer has also been investigated.

Results and Discussion

Previous studies have shown that the binding of Mn^{2+} to duplex DNA is primarily to the phosphates, with most of the binding being in the outer shell (Granot *et al.*, 1982b; Kennedy & Bryant, 1986). That is, there are intervening water molecules between the Mn^{2+} and the phosphate. A small percentage of the binding to phosphates may also be in the inner shell with direct phosphate–manganese interaction, without intervening water molecules. Mn^{2+} binding to the N7 of guanosine residues of duplex DNA has also been observed (Froystein *et al.*, 1993). In the DNA quadruplex structures studied here the N7 sites of the guanosine residues, with the exception of G8 in the 15mer aptamer, are involved in hydrogen bonding and are not available for interaction with Mn^{2+} . Thus, the resonances of the H8 protons of the guanosine residues in the quartet base-pairs cannot be broadened by scalar interactions induced by binding at N7, with the exception of G8 in the 15mer aptamer.

The binding of Mn^{2+} to nucleic acids can be monitored by EPR (Granot *et al.*, 1982a,b; Kennedy & Bryant, 1986; Reuben & Gabbay, 1975). When Mn^{2+} is bound to the DNA the correlation time increases, since the bound Mn^{2+} has the correlation time of the DNA (Granot *et al.*, 1982a,b; Kennedy & Bryant, 1986; Reuben & Gabbay, 1975). The increase in correlation time induces the EPR linewidths to increase and hence binding can be monitored by the Mn^{2+} EPR spectrum. An increase in linewidth represents a decrease in the amplitude of the EPR spectrum when shown in the first derivative mode of display (Granot *et al.*, 1982a,b; Kennedy & Bryant, 1986; Reuben & Gabbay, 1975). The titration of Mn^{2+} with the aptamer has been reported. The results showed that at a molar ratio of Mn^{2+} :DNA of 4:1 the intensity of the EPR spectrum is about half that of the spectrum of the sample of free Mn^{2+} .

When the molar ratio is 2:1 the intensity of the EPR spectrum is about 10% of that of free Mn^{2+} . Further addition of DNA reduces the intensity to near the noise level. The results on the dimer quadruplex were obtained with a total Mn^{2+} concentration of 10^{-5} M and analogous results were obtained at 5×10^{-6} M. The sensitivity of the EPR spectrometer did not allow data to be acquired at lower concentrations. The results on the dimer quadruplex are quite similar to those obtained on the aptamer and indicate that there are two binding sites.

These EPR results indicate that the binding constant of Mn^{2+} to both of these quadruplexes is $\approx 10^5 M^{-1}$, or larger, since all of the manganese is apparently bound when the molar concentration of the DNA is 5×10^{-6} M and the total concentration of Mn^{2+} is 10^{-6} M. The total phosphate concentration is $\approx 10^{-4}$ when the DNA concentration is 5×10^{-6} M so the binding constant for manganese binding to these quadruplex DNAs is $\approx 10^4 M^{-1}$, based on total phosphate concentration. The EPR results also indicate that there are two binding sites for each of the quadruplexes, since maximal broadening of the Mn^{2+} EPR signal is observed at a ratio of two Mn^{2+} per DNA, over a range of concentrations. The effects of ionic strength on the binding constant and number of binding sites were not determined since variations in the ionic conditions can induce the DNA to undergo conformational changes (Wang *et al.*, 1993a,b).

The refined solution structures of both DNAs were determined so as to be able to use the refined structures to allow comparison of the predicted and experimentally observed binding sites. The structures were refined as described above and the refined structures used to calculate the NOE spectra of the two quadruplex DNAs. The comparison of the experimental and predicted NOESY spectra is shown in Figures 2 and 3 and the refined structures are shown in Figures 4 and 5. It can be seen in both cases that the refined structures predict NOESY spectra that are in excellent agreement with the experimental data. Previously proposed structures for these two quadruplex DNAs (Schultze *et al.*, 1994a,b) also predict NOESY data in good agreement with the experimental data, with a few exceptions; the structures presented here give better agreement with the experimental results.

The location of the Mn^{2+} binding sites was determined by monitoring the proton NMR linewidths of the aptamer as the sample was titrated with Mn^{2+} . The protons close to the Mn^{2+} binding sites will be relaxed due to their proximity to the paramagnetic Mn^{2+} . The Mn^{2+} are in fast exchange on the NMR time scale as evidenced by the gradual increase in linewidths as the concentration of Mn^{2+} is increased. Previously we monitored the binding sites by observing the effects *via* one-dimensional proton spectra (Wang *et al.*, 1995). To obtain more information the higher resolution of two-dimensional NOESY spectra of the DNAs was exploited. The higher resolution of

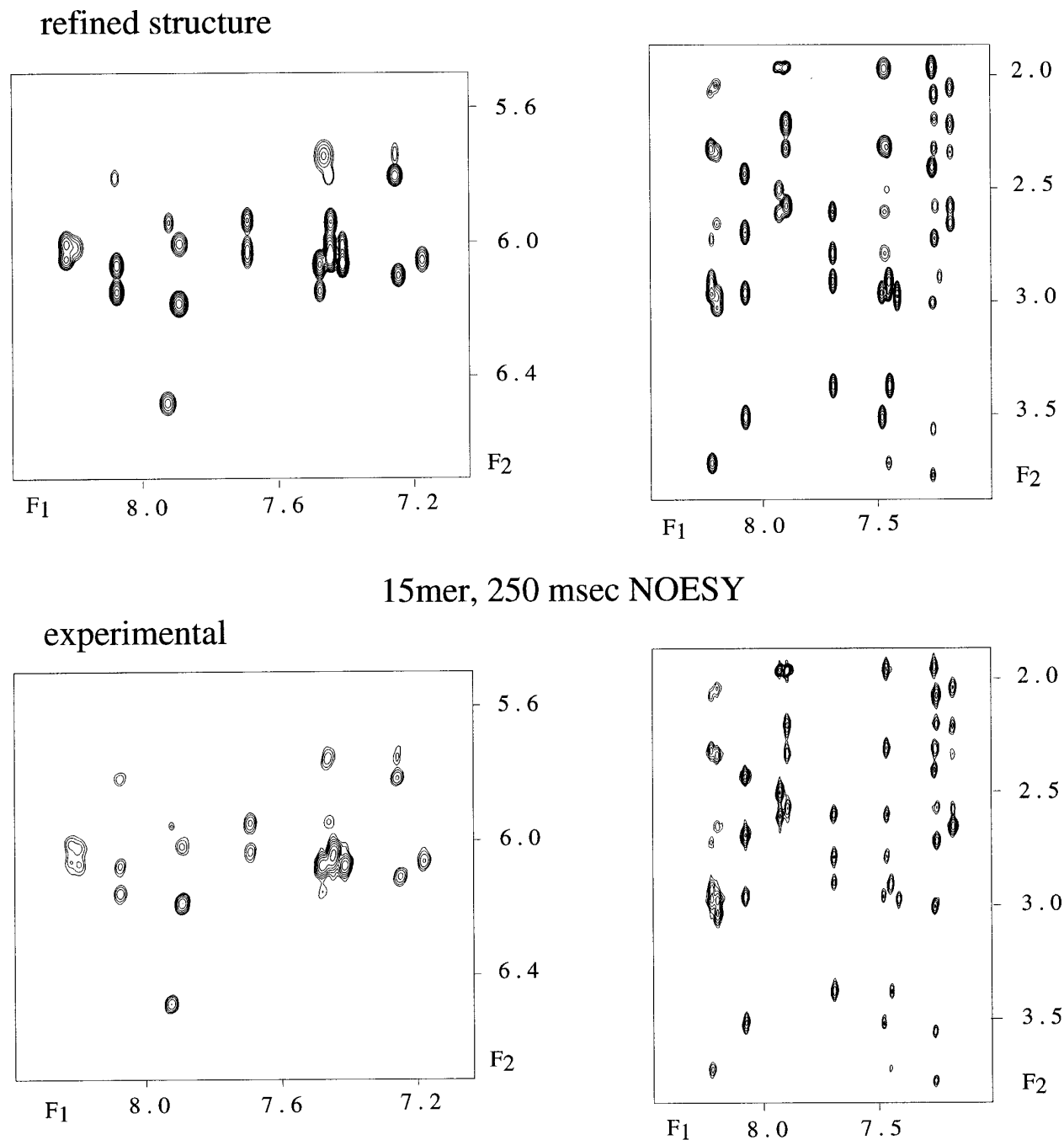
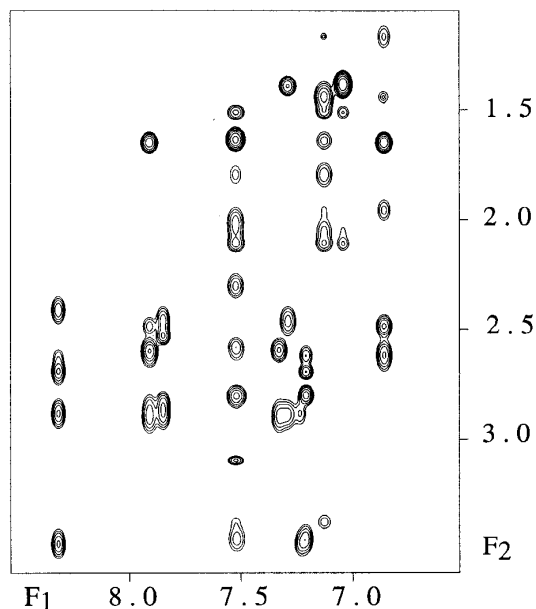
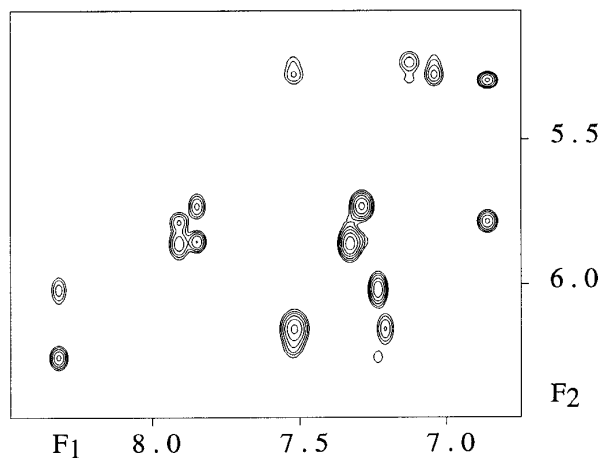


Figure 2. The NOESY spectra shown are those predicted by the refined solution structure of the 15mer and the experimental data. The spectra in the regions containing the cross-peaks of the aromatic and H1' protons as well as that of the aromatic and H2'/H2''/methyl protons are both shown.

the two-dimensional spectra allowed determination of about 20 constraints for each of the manganese sites on each of the quadruplex DNAs. Typical results from the manganese titration of the 15mer are shown in Figure 6 and for the dimer quadruplex in Figure 7. The locations of the bound manganese were determined from the enhanced relaxation data in much the same way as structures are determined from NOE data. That is, the enhanced relaxation results were

converted into distance constraints. More than 20 constraints were used to determine the location of each manganese ion and the positions determined satisfy all of the enhanced relaxation constraints. The experimentally determined manganese binding sites for the 15mer are shown in Figures 4 and 8, and for the dimer quadruplex in Figures 5 and 9, and these were determined without inclusion of DNA-Mn²⁺ electrostatic effects.

refined structure



12mer, 250 msec NOESY

experimental

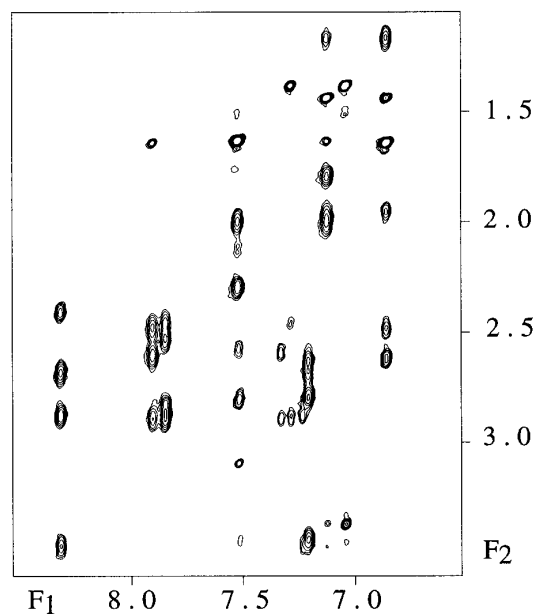
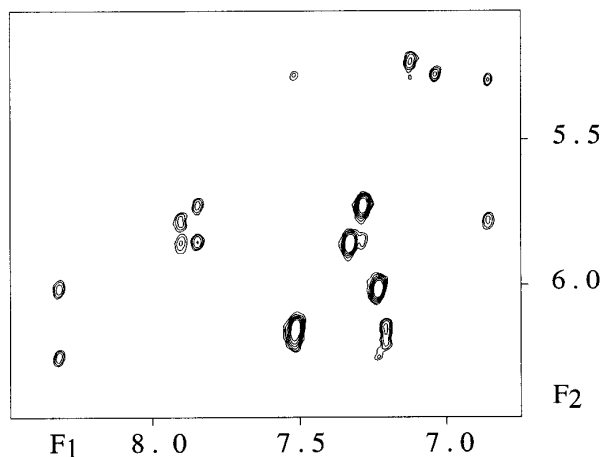


Figure 3. The NOESY spectra shown are those predicted by the refined solution structure of the 12mer and the experimental data. The spectra in the region containing the cross-peaks of the aromatic and H1' protons and the spectra in the region containing the aromatic and H2'/H2''/methyl protons are shown.

The structure of both quadruplexes predict that there will be strong Mn^{2+} binding sites in the narrow grooves. The electrostatic potentials on the surfaces of the two quadruplexes are shown in Figures 8 and 9. However, the manganese ions do not experience the electrostatic potential on the van der Waals' surface of the DNAs, since manganese

cannot approach so close to the DNA. The closest approach is the sum of the van der Waals' distances of the DNA and the manganese. The electrostatic potentials at approximately this distance are indicated by the grids in Figures 8 and 9. The locations of the manganese binding sites were predicted by holding the structures of the DNAs

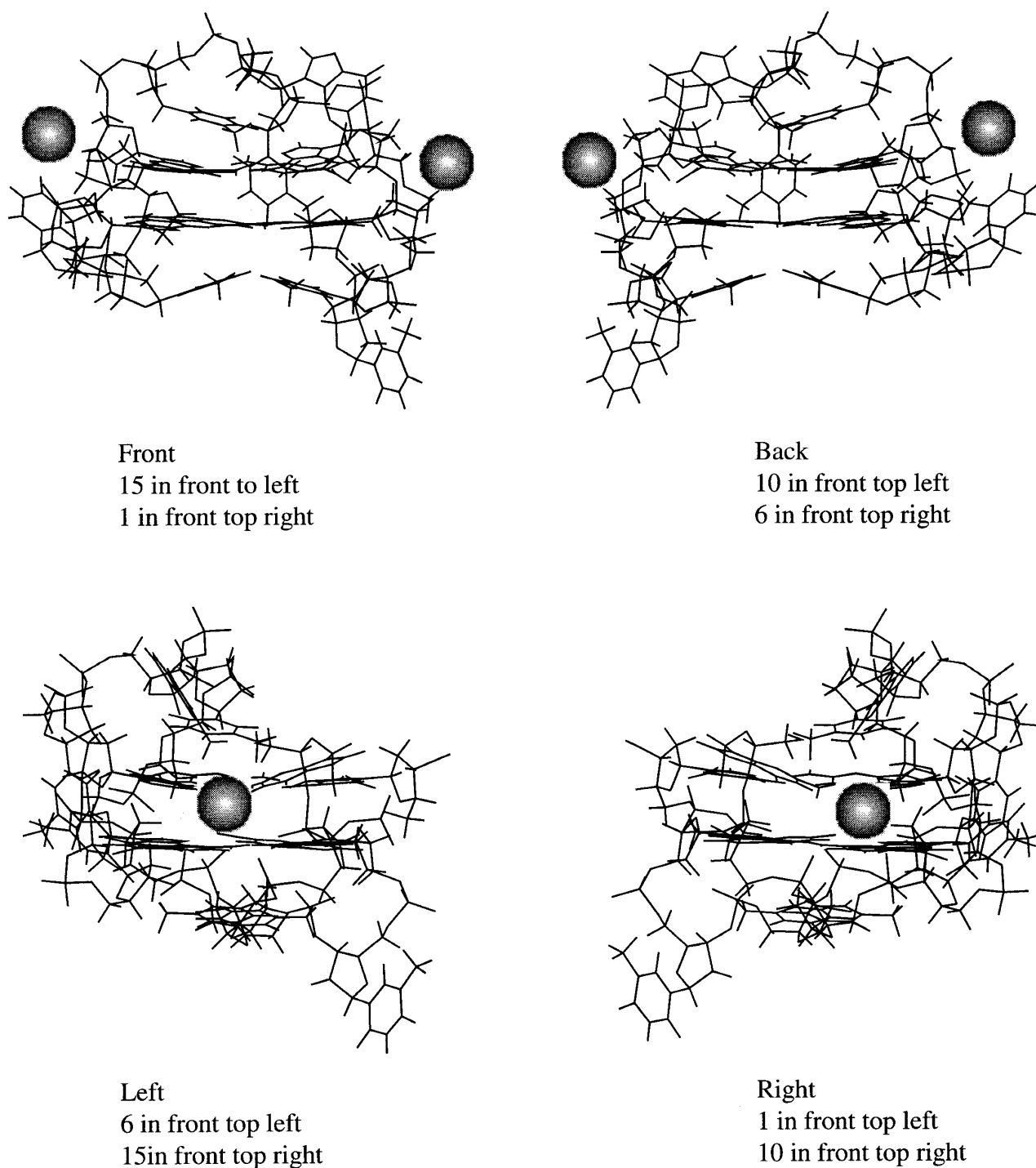
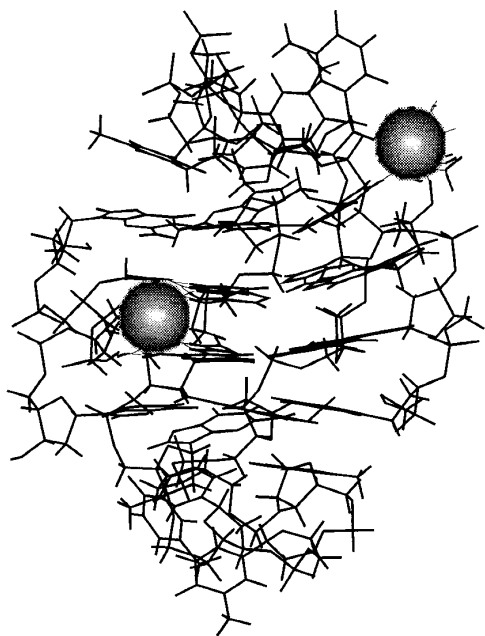


Figure 4. The refined solution structure of the 15mer is shown from four different perspectives. The front view has residue 1 in the top right and residue 15 in the top left. The back view has residue 10 in the top right and residue 6 in the top left. The left view has residue 15 in the top right and residue 6 in the top left. The right view has residue 6 in the top right and residue 1 in the top left. The front view corresponds to that shown in Figure 1. The experimentally determined positions of the manganese binding sites are also shown and indicated by the gray shaded spheres.

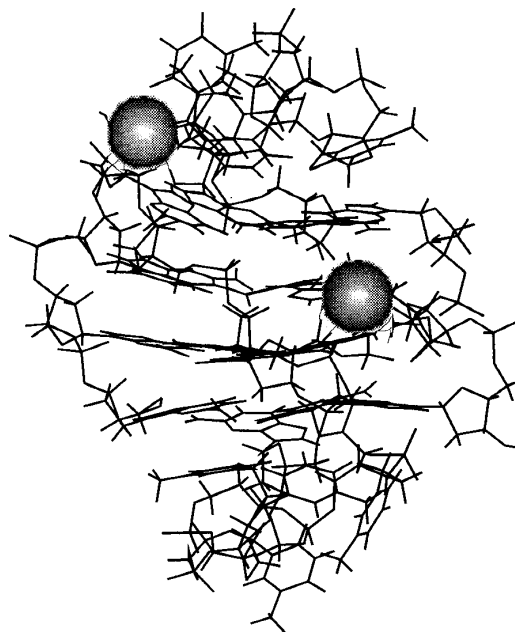
constant and finding the minimum energy positions for the manganese.

In the case of the aptamer one of the predicted manganese binding sites is very close (within 0.18 Å) to the experimentally determined site. The other predicted site, in the narrow groove adjacent to residues 1, 2, 5 and 6, is about 4.5 Å away from

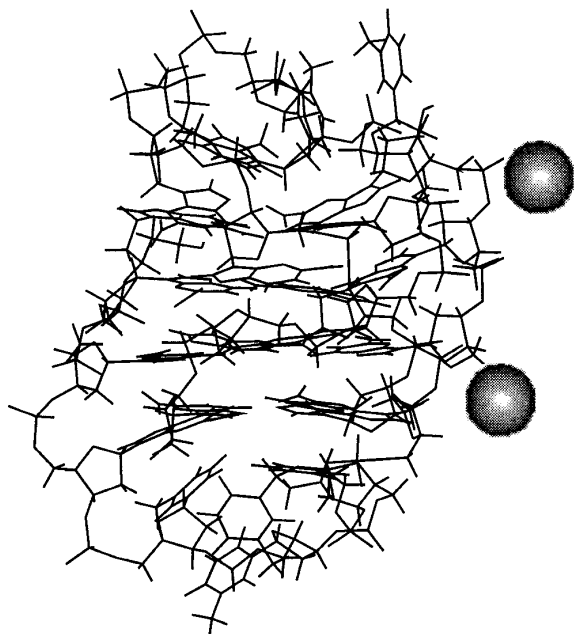
the experimentally determined site. While the predicted and experimental sites in this case are quite distinct in space they are very close in terms of electrostatic energy. The calculated energy for this experimental site is -6.465 kcal and for the corresponding predicted site is -6.915 kcal. The difference of ≈ 0.5 kcal is considered to be well



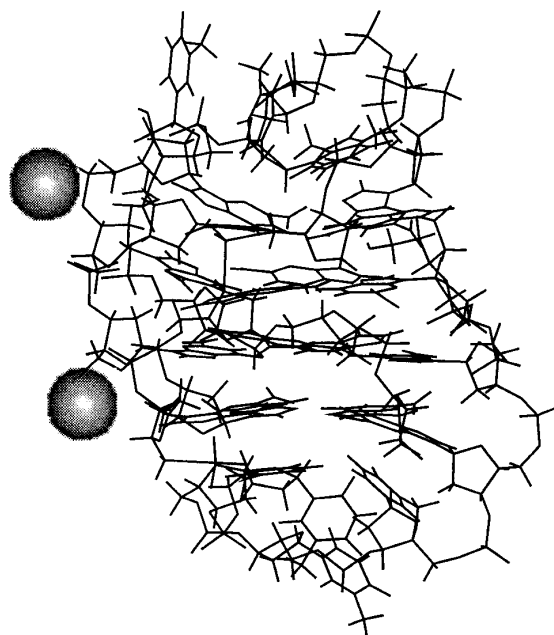
Front
9 in front top left
12 in front top right



Back
4 in front top left
1 in front top right



Left
1 in front top left
9 in front top right



Right
12 in front top left
4 in front top right

Figure 5. The refined solution structure of the 12mer is shown from four different perspectives. The front view has residue 12 in the top right and residue 9 in the top left. The back view has residue 1 in the top right and residue 4 in the top left. The left view has residue 9 in the top right and residue 1 in the top left. The right view has residue 4 in the top right and residue 12 in the top left. The back view corresponds to that shown in Figure 1. The experimentally determined positions of the manganese binding sites are also shown and indicated by the gray shaded spheres.

15mer, 250 msec NOESY

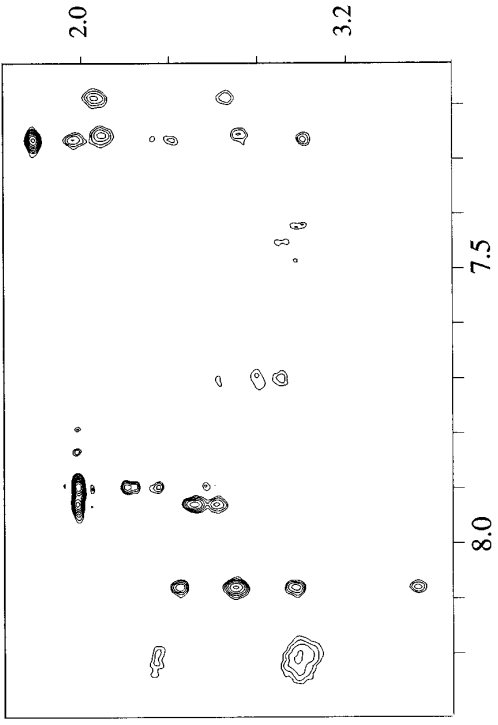
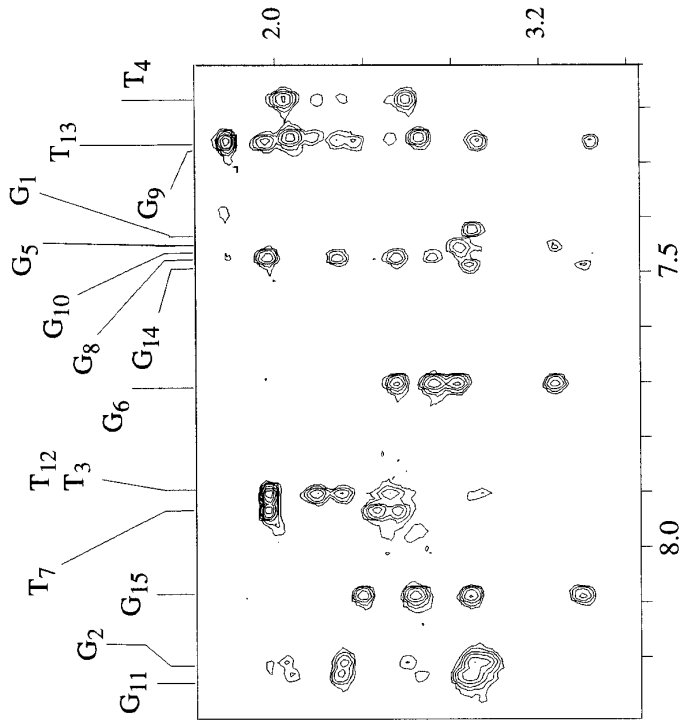
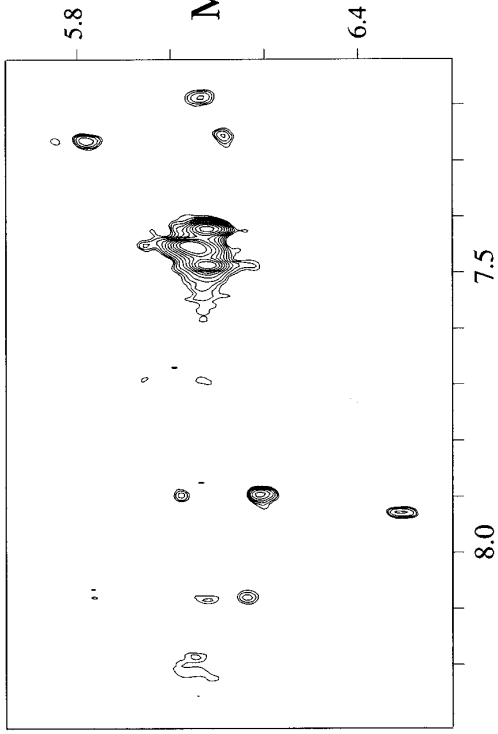
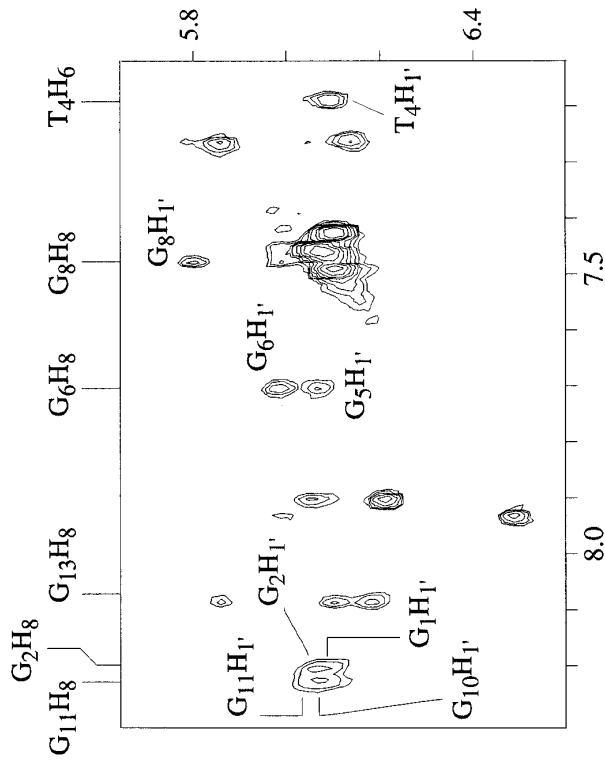


Figure 6. The 250 ms NOESY spectra of the 15mer obtained in the presence and absence of manganese are shown. The spectra in the region containing the cross-peaks of the aromatic and H1' protons and the spectra in the region containing the aromatic and H2'/H2''/methyl protons are shown. The assignments of some of the cross-peaks are indicated.

12mer, 250 msec NOESY

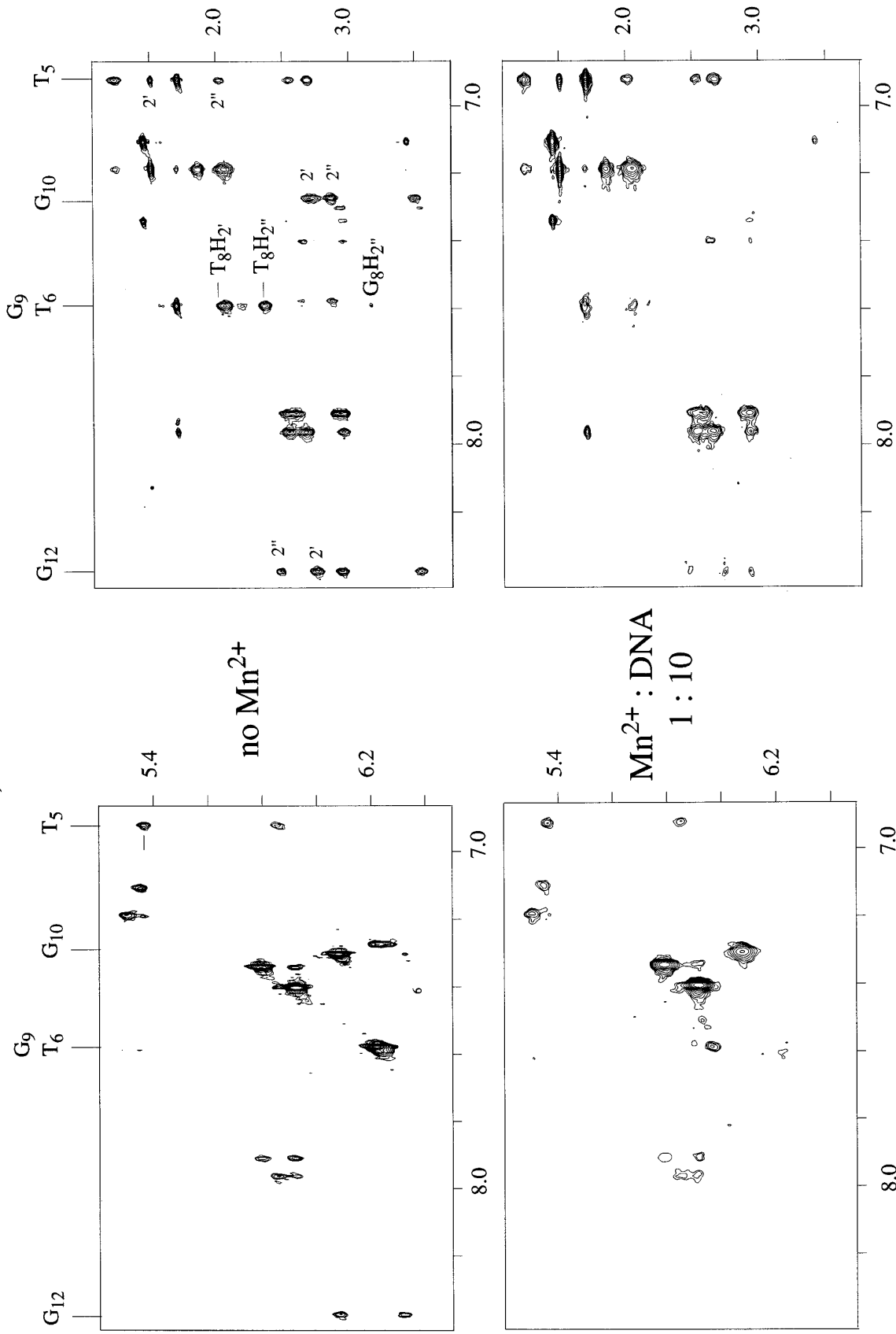


Figure 7. The 250 ms NOESY spectra of the 12mer obtained in the presence and absence of manganese are shown. The spectra in the regions containing the cross-peaks of the aromatic and H1' protons as well as that of the aromatic and H2'/H2''/methyl protons are shown. The assignments of some of the cross-peaks are indicated.

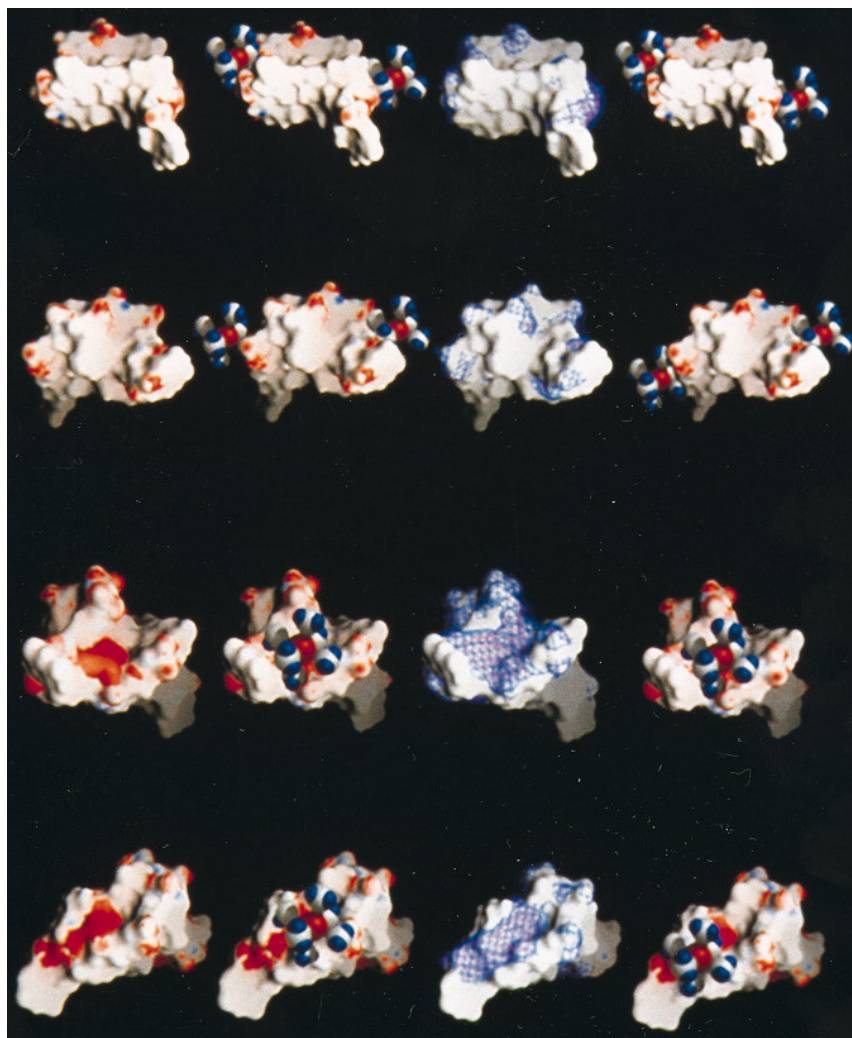


Figure 8. The left-most column shows the electrostatic potential on the surface of the 15mer with the front view at the top, then the back view, then the left view and the right view at the bottom. The second column from the left shows the electrostatic potential of the 15mer along with the experimentally determined position of the hydrated manganese binding sites. The hydrated manganese is shown in CPK mode. The third column shows the electrostatic potential surface between -6 and -7 kT in purple. The right-most column shows the electrostatic potential of the 15mer along with the predicted positions of the hydrated manganese binding sites.

within the accuracy of the prediction method. Figure 8 shows the electrostatic potential of the aptamer at -6 and -7 kT contour levels. It is seen that on the “left” side the highest negative potential has much less surface area than does the one on the “right” side. The difference of 0.5 kcal between the observed and predicted sites is good, considering the accuracy of the assumptions used to model the interactions.

The 15mer aptamer appears to have an additional, weaker binding site that is observed experimentally. The GH8 resonance of residue 8 is broadened at the higher levels of manganese. This broadening may be due to manganese binding to the N7 of this residue. G8 is the only guanine in the molecule that does not have its N7 involved in a hydrogen bond. Manganese binding to N7 is observed in DNA.

For the quadruplex formed of dimers of the 12mer an analogous comparison of the predicted and experimentally determined sites has been made. For this quadruplex both of the predicted sites are spatially and energetically close to those determined experimentally. For the site adjacent to residues 9B, 10B, 11A, 12A the distance difference

is 0.99 Å and the energetic difference is 0.37 kcal. The A and B strands are as defined in Figure 1. For the site adjacent to residues 9A, 10A, 11B and 12B the energetic difference is 0.47 kcal and the distance difference is 2.93 Å. Both sites on the dimer quadruplex have electrostatic potentials of similar magnitude to those found for the aptamer. Both sites are relatively well defined. It should also be noted that the region of high negative electrostatic potential is not a uniform ribbon through the narrow groove but the regions of highest negative electrostatic potential are well defined as indicated in Figures 8 and 9.

Since the Mn^{2+} are in fast exchange between being bound to the DNA and being free in solution, the binding sites determined here can be considered to be the “residence” sites. That is, these are the sites that the manganese ions preferentially occupy when bound to the DNA. When some peptides bind to proteins, for example, there may be significant conformational changes in the peptide that occur upon binding that can make determination of the bound state difficult. In this case there is at most a very small conformational change in the DNA induced by manganese binding,

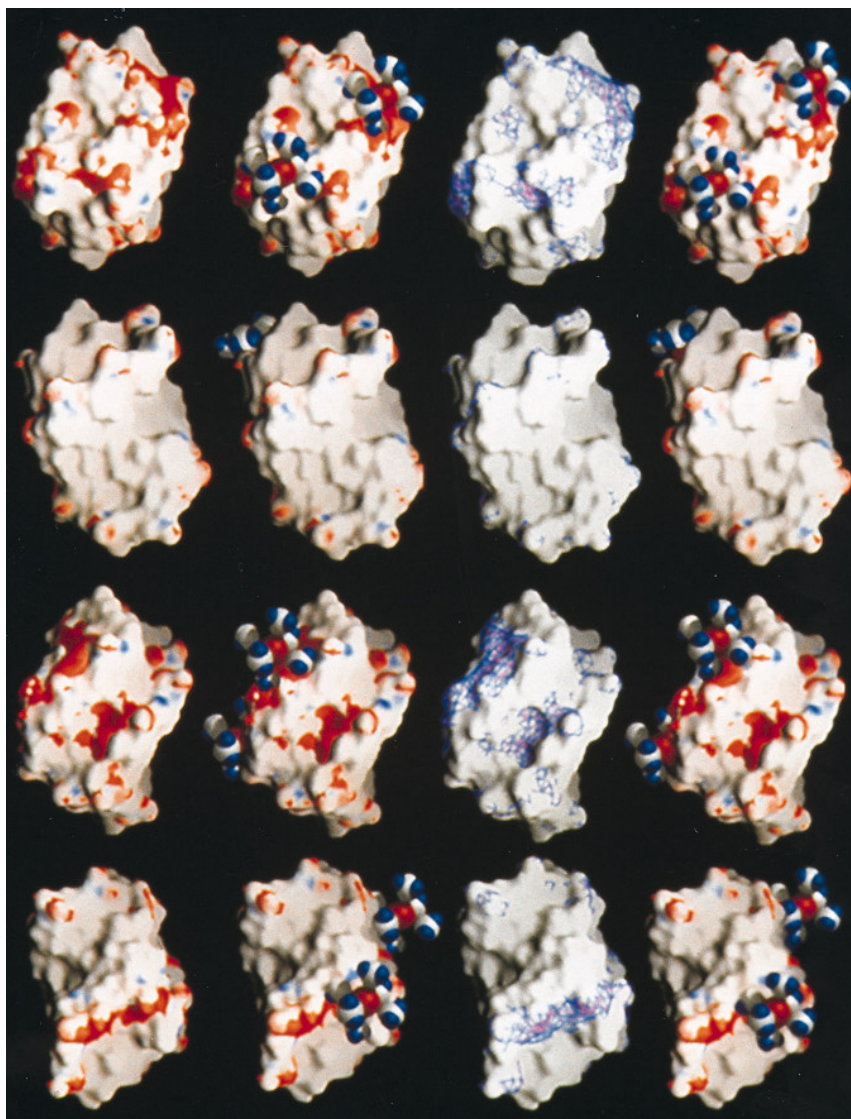


Figure 9. The left-most column shows the electrostatic potential on the surface of the 12mer with the front view at the top, then the back view, then the left view and the right view at the bottom. The second column from the left shows the electrostatic potential of the 12mer along with the experimentally determined position of the hydrated manganese binding sites. The hydrated manganese is shown in CPK mode. The third column shows the electrostatic potential surface between -8 and -9 kT in purple. The right-most column shows the electrostatic potential of the 12mer along with the predicted positions of the hydrated manganese binding sites.

so that the enhanced relaxation data can be used to determine the binding sites.

Once the binding sites of the free aptamer were determined experiments were carried out to determine if binding of the aptamer to thrombin restricts manganese binding. The binding constant of the aptamer to thrombin is 60 nM and hence much stronger than the binding of the aptamer to manganese (Wang *et al.*, 1993a). A sample of 10^{-4} M manganese was titrated with one aptamer per two manganese ions and the EPR first derivative signal decreased in intensity as shown in Figure 10. The sample was then titrated with thrombin, with the result that the first derivative EPR signal gained intensity. The gain in intensity indicates that thrombin binding releases both manganese ions from the aptamer. Since electrostatic effects are relatively short range these results indicate that thrombin binds to, or very close to, the same sites as does manganese. Thus, in the thrombin–aptamer complex both of the narrow grooves are apparently interacting with thrombin. A control titration showed that manganese does not

have significant interactions with thrombin at these concentrations that can be observed *via* EPR.

Experiments were carried out to examine the interactions between the dimer quadruplex and thrombin, with results shown in Figure 11. In this case the addition of thrombin to the quadruplex–manganese complex did not induce the release of manganese from the DNA. The addition of thrombin to the complex increased the intensity of the manganese signal by a small amount, which may be indicative of a weak interaction between the dimer quadruplex and thrombin. This result indicates that the dimer quadruplex does not bind to thrombin as well as the 15mer. This result also indicates that not all quadruplex structures bind to thrombin.

The refined solution structures of two quadruplex DNAs have been determined and these structures have been shown to be in excellent agreement with the NOESY and other data on the samples. These refined solution structures have been used to predict the locations of the binding sites of the paramagnetic ion manganese. For both

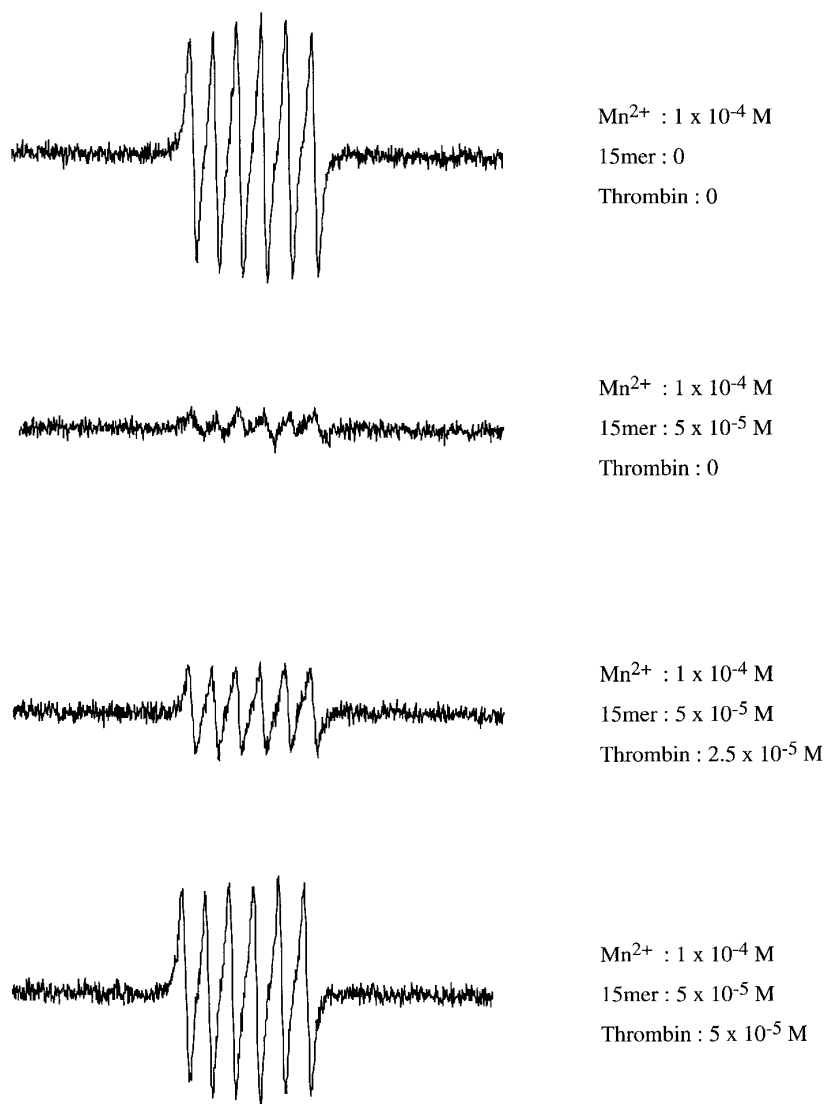


Figure 10. The EPR spectra obtained in the manganese–15mer–thrombin titration experiments are shown. The top spectrum is that of the free manganese. The next spectrum is that obtained when the 15mer is added to the manganese. The following spectrum is that of the manganese–15mer complex in the presence of a half stoichiometric amount of thrombin and the bottom spectrum is in the presence of a stoichiometric amount of thrombin.

DNAs the predicted and experimentally observed binding sites are very similar in terms of energy. The predicted binding sites and electrostatic potentials are consistent with the experimentally observed binding sites. However, the gradient of the electrostatic potential is too small in some locations for accurate prediction of the precise location of the binding site. For those sites with a relatively steep gradient the predicted and experimentally observed sites are close both in space and in energy terms. No assessment of mobility of the manganese while bound to the DNAs was made.

Once the location of the binding sites was known the binding of manganese to the DNAs was used to monitor their interaction with thrombin. The 15mer binds very strongly to thrombin. When the 15mer is bound to thrombin manganese binding is abolished, indicating that both narrow grooves are involved in the interaction of the 15mer with thrombin. This is consistent with a model previously proposed for the aptamer–thrombin complex (Wang *et al.*, 1993a). The quadruplex formed by dimers of the 12mer does not

appreciably associate with thrombin under the same conditions as does the 15mer. This is consistent with the 15mer–thrombin complex requiring a chair type structure for the quadruplex DNA. Analogous studies could be used to monitor other nucleic acid–protein interactions such as those of pseudoknot RNAs.

Experimental and Methods

The DNA aptamer, d(GGTTGGTGTGGTTGG), was prepared as described (Wang *et al.*, 1993b). A 100 A₂₆₀ DNA sample was dissolved in 0.6 ml of ²H₂O containing 140 mM NaCl, 5 mM KCl, and 20 mM perdeuterated Tris at pH 7.0. The extinction coefficient of the aptamer at 260 nm is 143,300 (Wang *et al.*, 1993a,b).

The DNA 12mer, d(GGGGTTTTGGGG), was prepared as described (Wang *et al.*, 1995). A 57 A₂₆₀ DNA sample was dissolved in 0.6 ml of ²H₂O containing 140 mM NaCl and 20 mM perdeuterated Tris at pH 7.0.

Each of the DNA samples was lyophilized and then dissolved in ²H₂O before the NMR MnCl₂ titrations. The titrations were over a range of DNA:Mn²⁺ ratios of 300:1 to 10:1 on a molar basis. No change in the chemical shifts

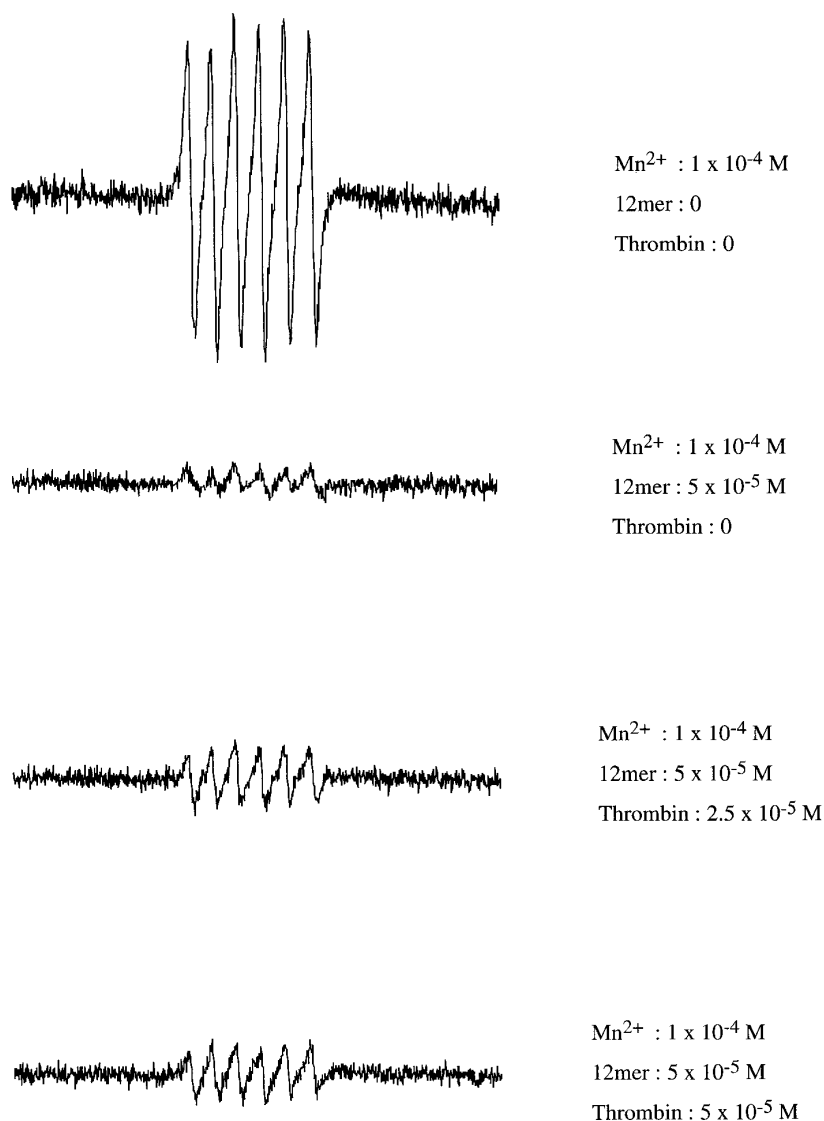


Figure 11. The EPR spectra obtained in the manganese–12mer–thrombin titration experiments are shown. The top spectrum is that of the free manganese. The next spectrum is that obtained when the 12mer is added to the manganese. The following spectrum is that of the manganese–12mer complex in the presence of a half stoichiometric amount of thrombin and the bottom spectrum is in the presence of a stoichiometric amount of thrombin.

of any DNA proton was observed during any of the Mn²⁺ NMR titrations, indicating that there was no Mn²⁺-induced structural change under the conditions used for these experiments.

The covalent active site inhibitor D-phenylalanine-proline-arginine chloromethyl ketone, (0.65 mg) was added to 10 mg of human thrombin ($M_r = 36,700$; Haematologic Technologies Inc.) essentially as described (Wang *et al.*, 1993a). Dialysis was conducted for seven days against a buffer solution of 46.7 mM NaCl, 1.67 mM KCl, 6.67 mM perdeuterated Tris, and 0.5 mM EDTA at pH 5.3 and 0°C. The dialysis was conducted in order to remove the glycerol and phosphates present in the thrombin sample and to remove any excess inhibitor.

All the NMR experiments were carried out on a Varian 400 Unityplus spectrometer. The NOESY spectra were carried out on samples in ²H₂O with a spectral width of 4000 Hz and with a 250 ms mixing time. A delay time of 1.8 seconds, a mixing time of 250 ms and 48 transients for each of the 360 increments of t_1 were used for the 12mer sample. A delay time of 2.0 seconds, a mixing time of 250 ms and 128 transients for each of the 390 increments of t_1 were used for the 15mer sample. The aptamer

sample was at 12°C for the NMR experiments and the dimer sample was at 20°C.

The EPR experiments were performed using a Bruker ESP 300 spectrometer. The spectra were obtained at band X with the sample in a flat quartz cell in a TE₁₀₂ cavity. The samples were at 20°C and the spectra were obtained with signal averaging of 20 transients.

Structure refinement

NOE cross-peak volumes and dihedral couplings were used as constraints in X-PLOR (Brünger, 1992) as described (Goljer *et al.*, 1995; Young *et al.*, 1995), with the following modifications. The structures of the quadruplexes were refined using a complete relaxation matrix restrained molecular dynamics trajectory, using X-PLOR. The force constants were the same as used for duplex DNA (Young *et al.*, 1995). The experimental NOE cross-peak volumes were used as constraints, using a well function. The experimental couplings were used to generate dihedral constraints defining sugar pucker and the conformation of the backbone using a harmonic

potential. In addition, constraints were used to keep the purine rings planar, as has been found to be the case for duplex DNA (Young *et al.*, 1995). The non-bonded interaction cut-off was set to 11.5 Å. The distance over which the switching functions for non-bonded interaction was switched from on to off was 9.5 to 10.5 Å. The distance cut-off for the hydrogen bonding interactions was set to 7.5 Å and the switching function was applied from 4.0 to 6.5 Å.

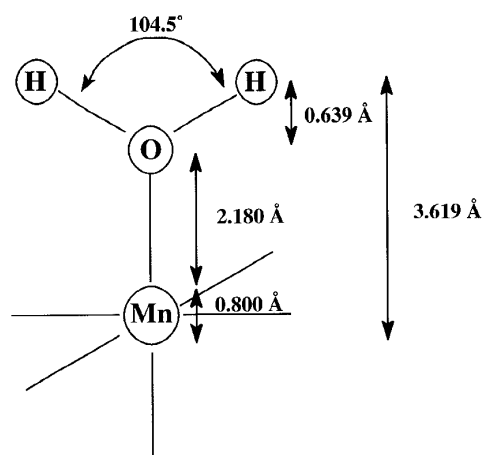
The starting structures were energy minimized by conjugate gradient minimization for 50 steps before starting the trajectories. The trajectory for the aptamer was run for 100 ps and that for the dimer for 40 ps. Each of the trajectories stabilized after about 20 ps. At the end of the trajectory the structures were subjected to an additional 200 steps of conjugate energy minimization. The final NOE rms, R and Q values (Withka *et al.*, 1992) for the aptamer are 0.14, 0.75 and 0.336, respectively, and for the dimer 0.29, 0.77 and 0.77.

For the aptamer 259 NOE volume constraints were used for each of the 100 and 250 ms mixing times. Eleven H1'-H2' dihedral constraints were used in addition to 13 H1'-H2'' dihedral constraints. Nine NOE constraints involving the imino protons of residues G1, G5, G6, G10, G14 and G15 were used.

For the dimer 350 NOE volume constraints were used for each of the 100 and 250 ms mixing times. Twenty four H1'-H2' dihedral constraints were used in addition to 22 H1'-H2'' dihedral constraints. Sixteen NOE constraints involving the imino protons of residues G1, G2, G4, G9, G10, G11 and G12 were also used.

Refinement of manganese binding sites

The refined structures of the two quadruplex DNAs were used along with X-PLOR 3.1 minimization protocols to determine the predicted sites of $[\text{Mn}(\text{H}_2\text{O})_6]^{2+}$ binding. The hexahydrate form of manganese was used, since the EPR evidence is consistent with the hexahydrate form and prior studies have all indicated that manganese interacts with nucleic acids as the hexahydrate in solution (Granot *et al.*, 1982a,b; Kennedy & Bryant, 1986; Reuben & Gabbay, 1975). In the crystal structure of $[\text{Mn}(\text{H}_2\text{O})_6]^{2+}$, the metal–oxygen distance is 2.18 Å (Montgomery, 1966; Shannon, 1976; Shannon & Prewitt, 1969). The overall radius of the hydrated complex is 3.619 Å and depends on the van der Waals' radius of the Mn^{2+} , the oxygen–hydrogen distance of water and the size of the water molecules as depicted below:



The A , B , ϵ and σ values of the Lennard-Jones potential were set to values appropriate for a sphere of this size. The attractive force is proportional to R^{-6} , and the repulsive force is proportional to R^{-12} . The values A , B and ϵ , σ are related to the well depth E_{min} and the minimum distance R_{min} is the van der Waals' radius: $R_{\text{min}} = \sigma(2)^{1/6}$; $E_{\text{min}} = -\epsilon$ (well depth); $A = 4\sigma^6\epsilon$; $B = 4\sigma^{12}\epsilon$; with $\sigma = 3.216$ Å and $\epsilon = 9.989 \times 10^{-7}$ kcal/mol as determined from the distances in the crystal structure.

Both quadruplex–manganese complexes were minimized using a 100-step rigid body minimization allowing only the hydrated manganese to move while the DNA was held rigid so that the structure of the DNA did not change during the minimization. The minimizations were run with various starting coordinates for the hydrated manganese. The final positions of the binding sites were found not to depend on the starting coordinates of the hydrated manganese and were not found to be particularly sensitive to the parameters discussed next. The distance cut-off for the hydrogen bonding interactions was set to 7.5 Å and the switching function was from 5.50 to 7.50 Å. The non-bonded interaction cut-off was set to 11.5 Å maximum and 1.5 Å minimum. The switching function for the non-bonded interactions was switched from active to non-active and was 9.5 to 10.5 Å. The distance-dependent dielectric function was also included in the non-bonded terms, with a value of 64. The charge on each hydrated manganese was set to +0.33.

The minimizations were carried out first with one manganese ion per quadruplex and then with two per quadruplex. The location of the first binding site did not change, upon addition of the second manganese, for either DNA.

Experimental determination of location of the binding sites

The enhanced relaxation of the protons is dependent on $1/r^6$, with r being the distance between the proton of interest and the manganese. Thus it seemed appropriate to use the enhanced relaxation as a distance constraint in the same manner as NOE information is used as a distance constraint in structure determinations. The enhanced relaxation of the protons was used to group the protons affected by the presence of manganese into three categories: strong (4.00 –1.10/+4.50 Å), medium (6.00 –1.10/+6.00), and weak (9.00 –3.00/+9.00) enhanced relaxation. These distance categories were arrived at by empirically minimizing the distance constraint violations. The positions of the binding sites were not found to be particularly sensitive to moderate changes in the distance bounds for the categories.

A total of 44 constraints were used in the aptamer calculations and 54 constraints for the 12mer calculations. The 44 NOESY cross-peaks used involved the following sites: G2H8, G6H8, G11H8, G1H2',H2'', T4H2',H2'', G5H2',H2'', G6H2',H2'', T12H2',H2'', and G14H2',H2'' as well as G5H3' were of the strong variety. G1H1', T4H1', T12H1', G2H2',H2'', G6H2',H2'', T9H2'/H2'', G11H2',H2'', and T4H6, G10H8, T13H6, and G15H8/H6 are of the medium type. T3H1',H2',H2'', G11H1',H2',H2'', G15H1',H2',H2'', T3H6, G5H8, T9H6, and G14H8 are in the weak group. The 12mer DNA is a dimer and the following apply to both strands unless stated otherwise. The 12mer DNA has G8H8, G9H8, G10H8, and G12H8, as well as G8H1',H2',H2'', G9H1',H2',H2'', G10H1',H2',H2'' in the strong group, as are G12H2'', G11H3', G9H3' and G9H5'. Those in the medium category are

G12H1', H2', H2" of both strands (except for G12H2"). In the weak group are G1H8, H1', H2'/H2", G2H8, H1', H2'/H2", G3H8, H1', H2'/H2", G4H8, H1', H2'/H2", T5H6, H1', H2'/H2", T6H6, H1', H2'/H2", T7H6, H1', H2'/H2", and G11H8, H1', H2'/H2".

These distance constraints were used in a 100 step Powell's conjugate gradient minimization using a 20 kcal/mol force constant for the distance constraints with a biharmonic potential, and the simulation was carried out at 300 K. Otherwise, the same X-PLOR parameters as used for the prediction of the manganese binding sites were used. The charge on each hydrated manganese was set to zero so that the minimization was based almost solely on the experimental data.

Models of electrostatic potentials

GRASP version 1.1 was used to model the electrostatic potentials of both the aptamer and dimer quadruplexes (Honig & Nicholls, 1995; Nicholls *et al.*, 1991). For both DNAs, the surface charges were calculated using the full charge option projecting neutral (white), negative (red) and positive (blue) areas on the molecular surfaces. The electrostatic potential cutoff for the aptamer was set to -9.0 kT and that of the 12mer -10 kT.

Grid type contours were calculated for the 15mer aptamer at -6.0 and -7.0 kT. The grid contours protrude from the molecular surface of the DNA, and hence represent the potential that the Mn^{2+} encounters at the van der Waals' contact distance from the quadruplex DNAs. Grid type contours for the 12mer had values of -8 and -9 kT.

Acknowledgements

The authors thank Dr T. David Westmoreland and Norriell Nipales for their assistance with the EPR experiments. The research at Wesleyan University was supported, in part, by grant GM 51298 from the National Institutes of Health. The NMR spectrometer was purchased with support from the National Science Foundation grant BIR 93-03077.

References

- Aboul-ela, F., Murchie, A. L. H. & Lilley, D. M. J. (1992). NMR study of parallel stranded tetraplex formation by the hexadeoxynucleotide d(TG₄T). *Nature*, **360**, 280–282.
- Blackburn, E. H. (1994). Telomeres: no end in sight. *Cell*, **77**, 621–623.
- Bock, L. C., Griffin, L. C., Latham, J. A., Vermass, E. H. & Toole, J. J. (1992). Selection of single stranded DNA molecules that bind and inhibit thrombin. *Nature*, **356**, 564–566.
- Brünger, A. T. (1992). *X-PLOR, Version 3.1*, Yale University Press, New Haven.
- Froystein, N. A., Davis, J. T., Reid, B. R. & Sletten, E. (1993). Sequence-selective metal binding to DNA oligonucleotides. *Acta Chem. Scand.* **47**, 649–657.
- Goljer, I., Kumar, S. & Bolton, P. H. (1995). Refined solution structure of a DNA heteroduplex containing an aldehydic abasic site. *J. Biol. Chem.* **270**, 22980–22987.
- Granot, J., Assa-Munt, N. & Kearns, D. R. (1982a). Interactions of DNA with divalent metal ions. IV. Competitive studies of Mn^{2+} binding to AT and GC-rich DNAs. *Biopolymers*, **21**, 873–883.
- Granot, J., Feigon, J. & Kearns, D. R. (1982b). Interactions of DNA with divalent metal ions. I. ^{31}P -NMR studies. *Biopolymers*, **21**, 181–201.
- Griffin, L. C., Tidmarsh, G. F., Bock, L. C., Toole, J. J. & Leung, L. L. K. (1993a). In vivo anticoagulant properties of a novel nucleotide based thrombin inhibitor and demonstration of regional anticoagulant extracorporeal circuits. *Blood*, **81**, 3271–3276.
- Griffin, L. C., Toole, J. J. & Leung, L. L. K. (1993b). The discovery and characterization of a novel nucleotide-based thrombin inhibitor. *Gene*, **137**, 25–31.
- Guschlbauer, W., Chantot, J. F. & Thiele, D. (1990). Four-stranded nucleic acid structures 25 years later: from guanosine gels to telomere DNA. *J. Biomol. Struct. Dynam.* **3**, 491–511.
- Hardin, C. C., Henderson, E., Watson, T. & Prosser, J. K. (1991). Monovalent cation induced structural transitions in telomeric DNAs: G-DNA folding intermediates. *Biochemistry*, **30**, 4460–4472.
- Hardin, C. C., Watson, T., Corregan, M. & Bailey, C. (1992). Cation dependent transition between the quadruplex and Watson–Crick hairpin forms of d(CGCG₃GCG). *Biochemistry*, **31**, 833–841.
- Honig, B. & Nicholls, A. (1995). Classical electrostatics in biology and chemistry. *Science*, **268**, 1114–1149.
- Kang, C., Zhang, X., Ratliff, R., Moyzis, R. & Rich, A. (1992). Crystal structure of four-stranded Oxytricha telomeric DNA. *Nature*, **356**, 126–131.
- Kennedy, S. D. & Bryant, R. G. (1986). Manganese-deoxyribonucleic acid binding modes. *Biophys. J.* **50**, 669–676.
- Laughlan, G., Murchie, A. I. H., Norman, D. G., Moore, M. H., Moody, P. C. E., Lilley, D. M. J. & Liusi, B. (1994). The high resolution crystal structure of a parallel stranded guanine tetraplex. *Science*, **265**, 520–524.
- Macaya, R. F., Scultze, P., Smith, F. W., Roe, J. A. & Feigon, J. (1993). Thrombin binding DNA aptamer forms a unimolecular quadruplex structure in solution. *Proc. Natl Acad. Sci. USA*, **90**, 3745–3749.
- Manning, G. S. (1978). The molecular theory of polyelectrolyte solutions with applications to the electrostatic properties of polynucleotides. *Quart. Rev. Biophys.* **11**, 179–246.
- Montgomery, H. (1966). The crystal structure of Tutton's salts. V. manganese ammonium sulfate hexahydrate. *Acta Crystallog.* **20**, 731–733.
- Nagesh, N., Bhargava, P. & Chatterji, D. (1992). Terbium-III induced fluorescence of four-stranded G4 DNA. *Biopolymers*, **32**, 1421–1424.
- Nicholls, A., Sharp, K. A. & Honig, B. (1991). Protein folding and association. Insights from the interfacial and thermodynamic properties of hydrocarbons. *Proteins*, **11**, 281–296.
- Record, M. T., Anderson, C. F. & Lohman, T. M. (1978). Thermodynamic analysis of ion effects on the binding and conformational equilibria of proteins and nucleic acids: the roles of ion association or release, screening, and ion effects on water activity. *Quart. Rev. Biophys.* **11**, 102–178.
- Reuben, J. & Gabbay, E. J. (1975). Binding of manganese(II) to DNA and the competitive effects of metal ions and organic cations. An electron paramagnetic resonance study. *Biochemistry*, **14**, 1230–1235.
- Ross, W. S. & Hardin, C. C. (1994). Ion-induced stabilization of the G-DNA quadruplex: free energy

- perturbation studies. *J. Am. Chem. Soc.* **116**, 6070–6080.
- Scaria, P. V., Shira, S. J. & Shafer, R. H. (1992). Quadruplex structure of d(G₃T₄G₃) is stabilized by K⁺ or Na⁺ as an asymmetric hairpin. *Proc. Natl Acad. Sci. USA*, **89**, 10336–10340.
- Schultze, P., Macaya, R. F. & Feigon, J. (1994a). Three-dimensional solution structure of the thrombin-binding DNA aptamer d(GGTTGGTGTG-GTTGG). *J. Mol. Biol.* **235**, 1532–1547.
- Schultze, P., Smith, F. W. & Feigon, J. (1994b). Refined solution structure of the dimeric quadruplex formed from the *Oxytricha* telomeric oligonucleotide d(GGGGTTTTGGGG). *Structure*, **2**, 221–233.
- Sen, D. & Gilbert, W. (1990). A sodium-potassium switch in the formation of four-stranded G₄-DNA. *Nature*, **344**, 410–414.
- Sen, D. & Gilbert, W. (1992). Guanine quartet structures. *Methods Enzymol.* **211**, 191–199.
- Shannon, R. D. (1976). Crystal structures of cations with coordination number six. *Acta Crystallog. sect. A*, **32**, 751–756.
- Shannon, R. D. & Prewitt, C. T. (1969). Crystal ionic radii of cations. *Acta Crystallog. sect. B*, **25**, 925–928.
- Shimmel, P. R. & Redfield, A. G. (1980). Transfer RNA in solution: selected topics. *Annu. Rev. Biophys. Bioeng.* **9**, 181–221.
- Smith, F. W. & Feigon, J. (1992). Quadruplex structure of *Oxytricha* telomeric DNA oligonucleotides. *Nature*, **356**, 164–168.
- Smith, F. W. & Feigon, J. (1993). Strand orientation in the DNA quadruplex formed from the *Oxytricha* telomere repeat oligonucleotide d(G₄T₄G₄) in solution. *Biochemistry*, **32**, 8682–8692.
- Smith, F. W., Lau, F. W. & Feigon, J. (1994). d(G₃T₄G₃) forms an asymmetric diagonally looped dimeric quadruplex with guanosine 5'-syn-syn-anti and 5'-syn-anti-anti N-glycosidic conformations. *Proc. Natl Acad. Sci. USA*, **91**, 10546–10550.
- Wang, K. Y., Krawczyk, S. H., Bischofberger, N., Swaminathan, S. & Bolton, P. H. (1993a). The tertiary structure of a DNA aptamer which binds to and inhibits thrombin determines activity. *Biochemistry*, **32**, 11285–11295.
- Wang, K. Y., McCurdy, S., Shea, R. G., Swaminathan, S. & Bolton, P. H. (1993b). A DNA aptamer which binds to and inhibits thrombin exhibits a new structural motif for DNA. *Biochemistry*, **32**, 1899–1904.
- Wang, K. Y., Swaminathan, S. & Bolton, P. H. (1994). Tertiary structure motif of *Oxytricha* telomere DNA. *Biochemistry*, **33**, 7517–7527.
- Wang, K. Y., Gerena, L., Swaminathan, S. & Bolton, P. H. (1995). Determination of the number and location of the manganese binding sites of DNA quadruplexes in solution by EPR and NMR. *Nucl. Acids Res.* **23**, 844–848.
- Wang, Y. & Patel, D. J. (1992). Guanine residues in d(T₂AG₃) and d(T₂G₄) form parallel-stranded potassium cation stabilized G-quadruplexes with anti glycosidic torsion angles in solution. *Biochemistry*, **31**, 8112–8119.
- Wang, Y. & Patel, D. J. (1993). Solution structure of the human telomeric repeat d[AG₃(T₂AG₃)₃] G-tetraplex. *Structure*, **1**, 263–282.
- Wang, Y., Jin, R., Gaffney, B., Jones, R. A. & Breslauer, K. J. (1991). Characterization by ¹H NMR of glycosidic conformations of the tetramolecular complex formed by d(GGTTTTGG). *Nucl. Acids Res.* **19**, 4619–4622.
- Williamson, J. R. (1993). G-quartets in biology: reprise. *Proc. Natl Acad. Sci. USA*, **90**, 3124–3124.
- Williamson, J. R., Raghuraman, M. K. & Cech, T. R. (1989a). Monovalent cation induced structure of telomeric DNA: the G quartet model. *Cell*, **59**, 871–880.
- Williamson, J. R., Raghuraman, M. K. & Cech, T. R. (1989b). Monovalent cation-induced structure of telomeric DNA: the G-quartet model. *Cell*, **59**, 871–880.
- Withka, J. M., Srinivasan, J. & Bolton, P. H. (1992). Problems with, and alternatives to the NMR R factor. *J. Magn. Reson.* **98**, 611–616.
- Wyatt, J. R., Puglisi, J. D. & I. Tinoco, J. (1990). RNA pseudoknots. Stability and loop size requirements. *J. Mol. Biol.* **214**, 455–470.
- Young, M. A., Beveridge, D. L., Goljer, I., Kumar, S., Srinivasan, J. & Bolton, P. H. (1995). Structure determination and analysis of local bending in an A-tract DNA duplex: Comparison of results from crystallography, nuclear magnetic resonance and molecular dynamics simulation on d(CGCAAAAATGCG). *Methods Enzymol.* **261**, 121–144.

Edited by I. Tinoco

(Received 12 January 1996; received in revised form 16 April 1996; accepted 24 April 1996)